New Trends in Mathematical Physics (November 7–12, 2022)
Steklov International Mathematical Center
Steklov Mathematical Institute of Russian Academy of Sciences, Moscow

Holographic interface of activated heterostructures with 2D Fermi gas. Internal processes in betavoltaic SiC obtained by CVD technology

Mikhail V. Dolgopolov[1,2], M. V. Elisov[2], A. V. Gurskaya[1,2]

[1] SAMARA POLYTECH & [2] Samara University, Russia

November 9, 2022. Slides of abstracts

Introduction/ Motivation

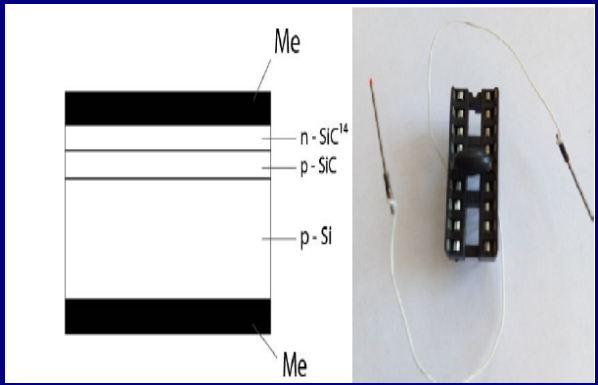

Since 2015-2017, several new types of devices for converting beta decay energy into electrical energy and research groups have appeared in the world, developing these beta converters. The basis is the semiconductor structure which is capable of optimal (and cheap) direct converting the energy of beta radiation of the radionuclide as the "INNER SUN" into the external electric current.

High Lights / Interface aspects, thin layers

1. Description of criteria for the formation of semiconductor heterostructures on silicon with sharp barrier transitions with accumulation of 2DEG during activation of splitting of quasi-Fermi levels by radiation sources.
2. By means of inversion, the large density of electron and/or hole 2D gas is created. The possibilities of optimization by doped modulation of graded heterojunction and quasi-electric built-in field in the technological process of endotaxy of thin films into silicon are determined.
3. Optimization is carried out according to the parameters of the band gap width and concentrations of alloying impurities for I(V).
4. The conditions of physical separation of 2D Fermi gas from impurity in the depletion mode with low scattering of interface roughness, which leads to high carrier mobility.

Growth of structures in the endotaxy process

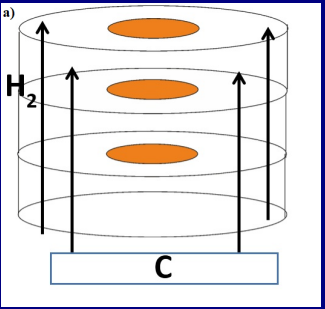

Figure 1: A distribution scheme of silicon substrates in gas camera

Endotaxy is the new phase growth process within another. We are considering now cubic phase of 3C-SiC on a silicon substrate. Radionuclide C-14 is implemented instead of C-12 in the SiC phase in the por or nonpor SiC/SiC/Si heterostructure during endotaxy. The concept is based on the solid-phase transformation from the Si-phase to the SiC-phase, which allows the C-14 accumulation in the por-Si phase of the heterostructure. The endotaxy process is carried out in the hydrogen flow.

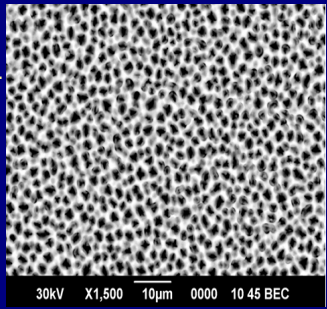

Figure 2: Porous structure of SiC obtained by CVD technology

Growth of structures in the endotaxy process

The Silicon Carbide grows due to the Carbon precipitation gradient (the Carbon concentration in the surface layers is above the solubility limit) and the formation of a compound with the Si phase.
Two stages take place: 1) $C + 2H_2 \leftrightarrow CH_4$, 2) $CH_4 + Si \rightarrow SiC + 2H_2$

Figure 3: Photo of the CVD reactor

We should note also that doping to obtain p- or n-types of conductivity is also performed in the CVD reactor specially designed for research. Ultimately, the structure contains a radionuclide as an energy source in the potential birthplace of electrons and holes. This place is the SCR.

Measurements of physical characteristics

The results of measuring current and voltage for three samples in two cases are interesting: 1) in the case of an additional light source; 2) in the dark. These three heterostructures differ in the sequence of layer build-up in the CVD reactor, as well as the type of semiconductor structure in the result of doping. We observe a light current in all three cases. We also register a current in the absence of light, the so-called dark current. And this convincingly demonstrates the betaconverter operability.

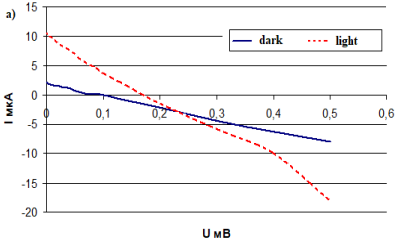

Figure 4: N-SiC/P-Sic/p-Si

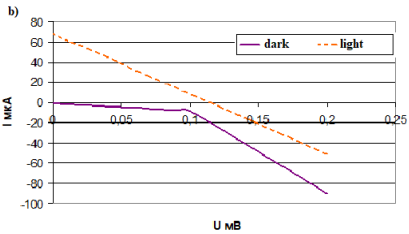

Figure 5: Ni/P-SiC/p-Si

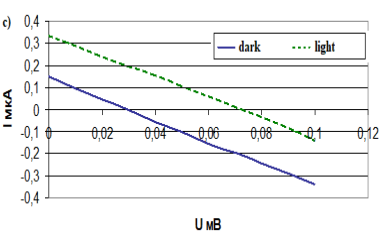

Figure 6: P-SiC/p-Si

Diffusion and structural evolution of 3C-SiC/Si

Due to the development of the capabilities of computer technologies and methods of quantum chemistry, we have engaged DFT for the analysis of the 3C-SiC phase with alloying atoms: P, Ga and N. The main goal was to estimate the value of the band gap as a function of the amount of doped atom in 3C-SiC. These values can only be compared with each other within the model, but not with experimental data, because the band gap width in DFT calculations is slightly lower than in real measurements.

Table 1: The band gap width for the 3C-SiC cell (12 atoms) with a different number of doped atoms instead C-12. [M.V. Dolgopolov et al. Journal of Physics: Conference Series 1686(1) (2020) 012040]

Model	SiC	+1Ga	+2Ga	+3Ga	+1P	+2P	+3P	+1N	+2N	+3N
E_g, eV	1.36	1.57	1.87	1.95	1.90	1.67	0.97	2.02	3.88	1.73

Diffusion and structural evolution of 3C-SiC/Si

The energy of cell formation was recalculated as the binding energy per 1 atom according to the formula:

$$E_b = \frac{E_m - E_d N_d - E_{SiC} N_{SiC}}{N_d + N_{SiC}}, \qquad (1)$$

where E_m - energy of pure model cell,
N_d, N_{SiC} - numbers of atoms in cells of pure substance,
E_d, E_{SiC} - energy of pure substance cells.

Calculations were carried out using the VASP application with PBE potentials in a basic set of plane waves. Energy cutoff is 600 eV. The length in the reciprocal space is 15 A.

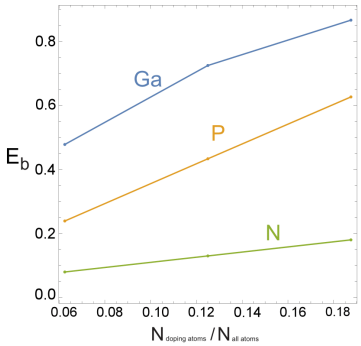

Diffusion and structural evolution of 3C-SiC/Si

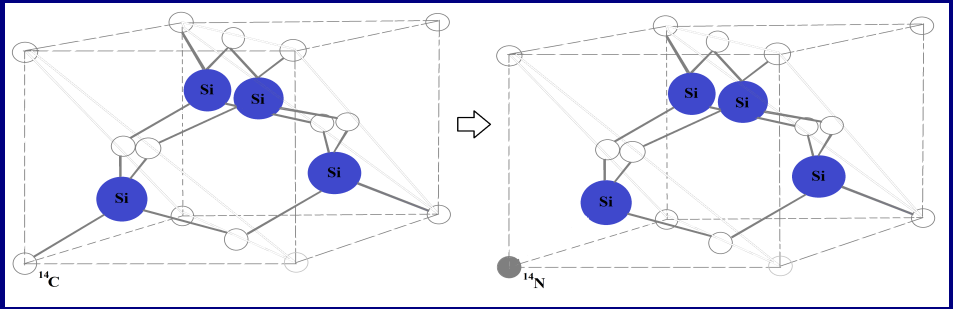

Figure 8: The loss of the bond of the nitrogen atom after the C-14 decay

The atom N-14 does not belong to the cell, so it can leave its position. And the vacancy can be filled with other atoms from the immediate environment. We assume that the diffusion of C-atoms can be continued. And C-14 will be moved too.

Generation of electrons

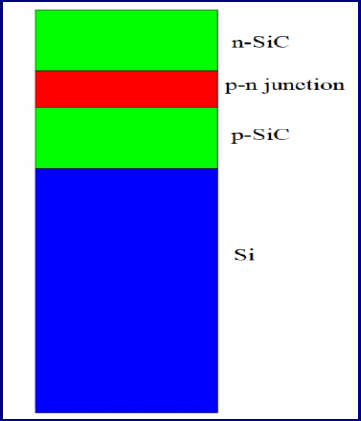

Figure 9: Model of beta-converter in GEANT4

We expect that the existence of an electric field in the SCR is the main source of charges separation. So, we have realized the simulation in the framework of GEANT package.The program allowed us to put the so-called "detectors" of electrons were placed at the distance of 1 μm from each other as they deepened. The result that the optimal depth of the p–n junction is directly below the N-SiC layer with C-14. [M.V.Dolgopolov et al EPJ Web of Conferences 222, 02012 (2019)]

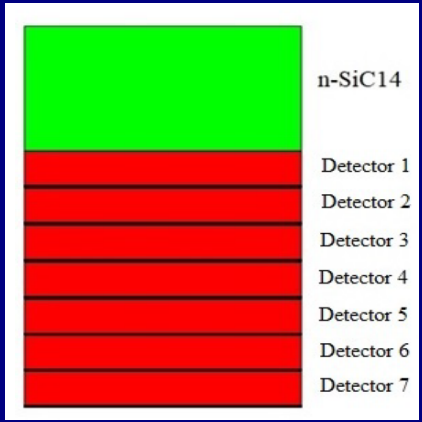

Figure 10: Model made to determine the optimal depth of the p-n junction

Theoretical description of endotaxy process

There were theoretical calculations of the depth of the position of the p-n junction in the Silicon Carbide structures grown in this reactor. However, the study was limited to the well-known C-12, the behavior of which does not differ from C-14. The diffusion of alloying impurities was considered in the form of a system of equations. Here we can expect that the depth of the p-n junction is 2 μm (see Fig.10).

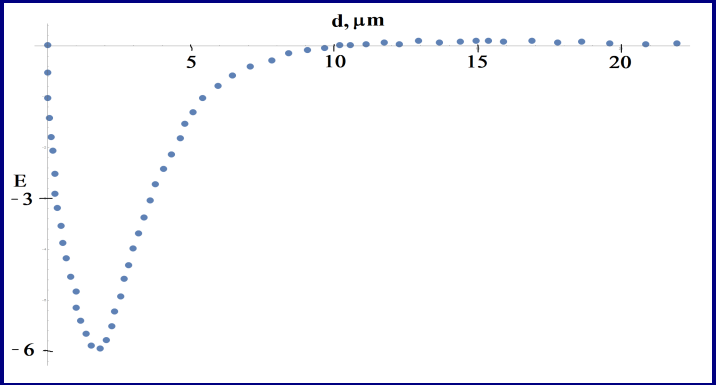

Figure 11: Dependence of the electric field strength on the depth. The value of the strength 6 corresponds to the absolute value of the internal electric field $E \sim 10^5$ V/m.

Avalanche Photodiode

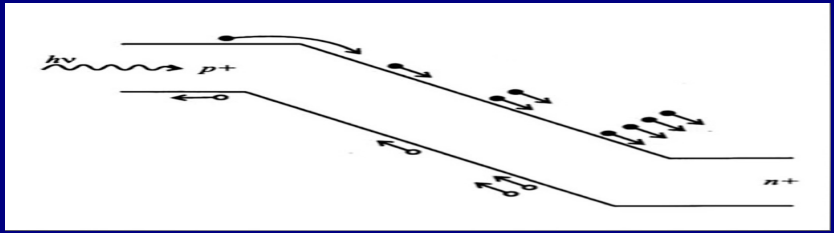

When reverse bias is large, the photodiode may experience impact ionization and avalanche breakdown. Single high energy electron can produce many electrons and holes through avalanche breakdown process - Produces gain - Effective low light level detector

Avalanche Breakdown

Assume an = ap to find:

$$n_f - n_0 = n_f \int_{x_a}^{x_c} \alpha \, dx \quad \Rightarrow \quad M \equiv \frac{n_f}{n_0} = \left[1 - \int_{x_a}^{x_c} \alpha \, dx \right]^{-1}$$

- M diverges when $\int_{x_a}^{x_c} \alpha \, dx = 1$ breakdown! - This condition means that for an electron entering the interval Xa Xc the probability of impact ionization is 1. - Single electron entering the depletion region causes indefinite current. If ap = 0,

$$\frac{dn}{dx} = \alpha_n n \quad \Rightarrow \quad M = \frac{n_f}{n_0} = \exp\left[\int_{x_a}^{x_c} \alpha \, dx \right] \quad : \text{no breakdown}$$

Superlattice Avalanche Photodiode

Upon entering the narrow bandgap layer from a wide bandgap layer, electrons gets a boost in their kinetic energy due to the conduction band discontinuity. Even if the overall applied field is lower than the threshold field in the bulk material, impact ionization events can still take place in the vicinity of the band discontinuity.

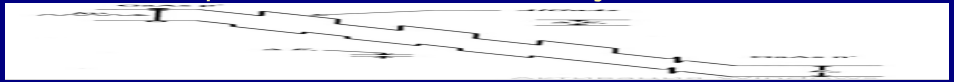

drawing slide

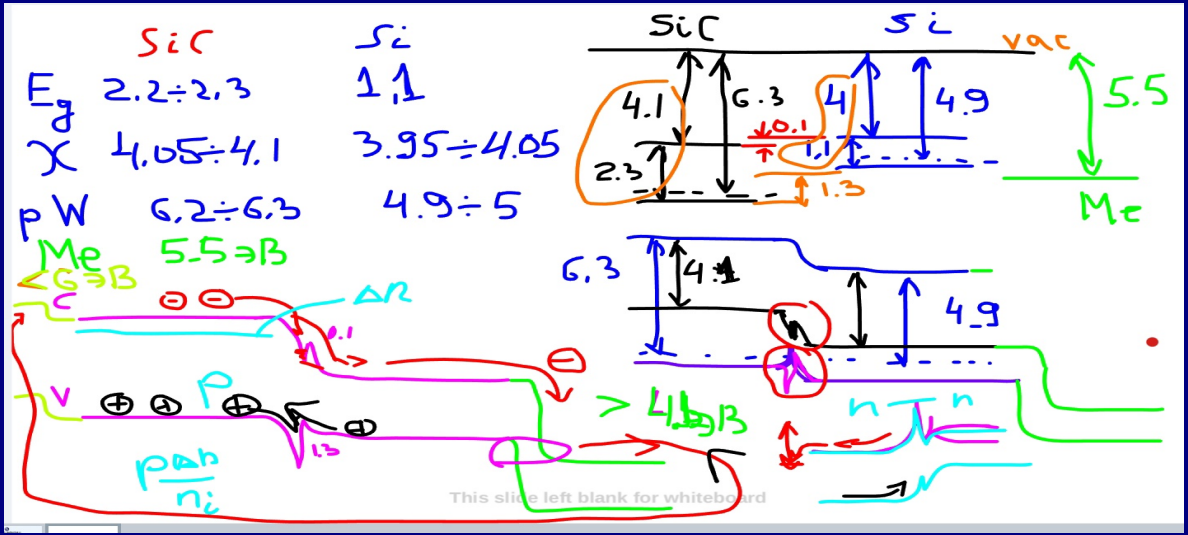

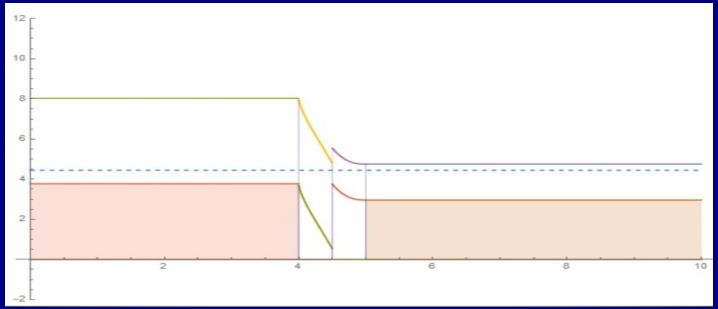

$$\Delta E_c = \chi_{\mathrm{Ge}} - \chi_{\mathrm{GaAs}}.$$

$$\Delta E_v = \left(\chi_{\mathrm{Ge}} + E_{g\,\mathrm{Ge}}\right) - \left(\chi_{\mathrm{GaAs}} + E_{g\,\mathrm{GaAs}}\right) = \Delta E_c + \left(E_{g\,\mathrm{Ge}} - E_{g\,\mathrm{GaAs}}\right).$$

$$\Delta E_c + \Delta E_v = E_{g\,\mathrm{Ge}} - E_{g\,\mathrm{GaAs}}$$

Fermi gas

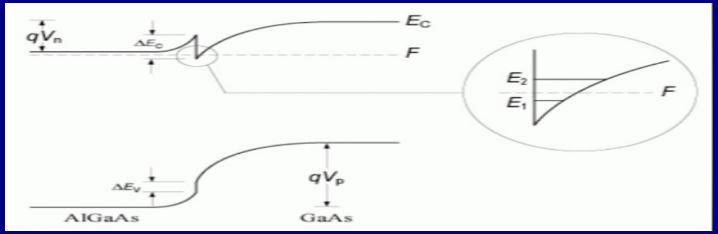

Band diagram of a heterojunction illustrating two-dimensional quantization

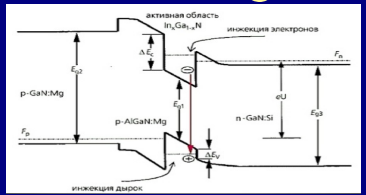

AlGaN quantum well formed in an InxGa1-xAs/GaN layer

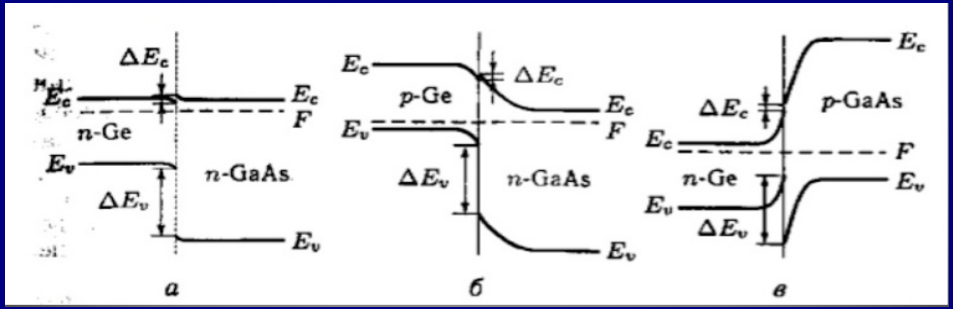

Idealized Energy Diagrams of Heterojunctions Ge–GaAs: (a) isotype nn heterojunction; b, c – anisotype pn- and np-heterojunctions

Quasi-Fermi levels

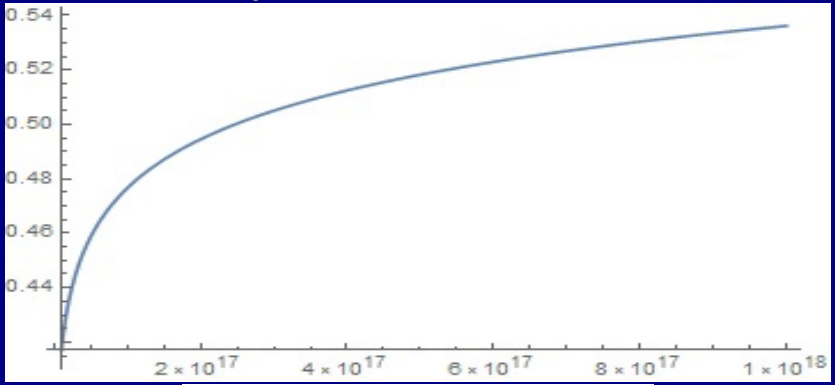

$$f_n = \left(1 + \exp\left(\frac{E - F_n}{kT}\right)\right)^{-1}.$$

Haos in semiconductors

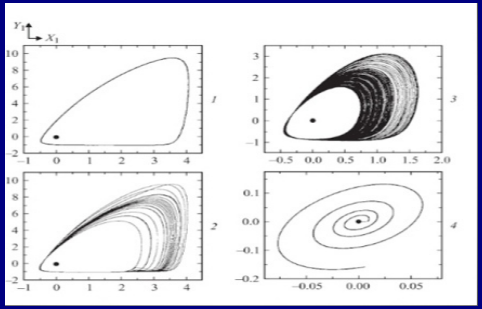

The impurity electrical breakdown of a compensated semiconductor is one of the mechanisms favoring the appearance of vibrational instability. When a magnetic field is applied, chaotic self-oscillations can be obtained.

Haos in semiconductors

$$\frac{dn_1}{dt} = \gamma_{op}[N_D - N_A - n_1] + A_I^{(1)}(Z_1)[N_D - N_A - n_1]n_1$$
$$- B_T^{(1)}(Z_1)[N_A + n_1]n_1,$$
$$\frac{dn_2}{dt} = \gamma_T[N_D - N_A - n_2] + A_I^{(2)}(Z_2)[N_D - N_A - n_2]n_2$$
$$- B_T^{(2)}(Z_2)[N_A + n_2]n_2,$$
$$\frac{dE_1}{dt} = \frac{4\pi}{\varepsilon SR}\left[\mathscr{E} - E_1 L - E_2 L - eSRn_1\mu_1(Z_1)E_1\right],$$
$$\frac{dE_2}{dt} = \frac{4\pi}{\varepsilon SR}\left[\mathscr{E} - E_2 L - E_1 L - eSRn_2\mu_2(Z_2)E_2\right],$$

To analyze the model, we will compose the following system of equations for the concentrations and strengths of electric fields.

Conclusion and future development

1. We have received reliable confirmation of the beta converter operation for the cubic structure of Silicon Carbide obtained as the phase on the silicon substrate surface during the endotaxy.
2. We were convinced of the plausibility of the movement of atoms in vacancies.
3. The introduction of activation by the source makes it possible to spread the quasi-Fermi levels to the effect of superinjection at the interface when n quasi-levels are raised above the bottom of the conductivity and p below the valence, which increases the concentration higher than that of n and p semiconductors, and this is equivalent to an effective double heterojunction with the very thin layer up to 10 atomic sizes, in which superinjection of electrons and holes is manifested, and there is no Fermi level.
4. It is important to physically separate the Fermi gas concentrations and impurities to avoid recombination. Holographic interface is need...
5. Created barriers for the diffusion current when the circuit is closed, taking into account the corresponding metallization.

Thanks for your attention!